Physica B 646 (2022) 414327

Contents lists available at ScienceDirect

Physica B: Physics of Condensed Matter

journal homepage: www.elsevier.com/locate/physb

Spectroscopic properties of Nd^{3+}-doped boro-bismuth glasses for laser applications

K. Udaya Kumar [a], P. Babu [b], Ch. Basavapoornima [c], R. Praveena [d], D. Shobha Rani [c], C.K. Jayasankar [a,*]

[a] Department of Physics, Sri Venkateswara University, Tirupati- 517 502, India
[b] Department of Physics, NTR Government Degree College, Vayalpad- 517299, India
[c] Institute of Aeronautical Engineering, Hyderabad, 500 043- India
[d] Department of Physics, Gayatri Vidhya Parishad College of Engineering (A), Visakhapatnam- 530048, India

ARTICLE INFO

Keywords:
Nd^{3+}-doped glasses
Boro-bismuth glasses
Judd-Ofelt analysis
Radiative properties
Near-infrared emission
Rare earths

ABSTRACT

Trivalent neodymium (Nd^{3+})-doped boro-bismuth glasses have been prepared adopting the high temperature melt and quick quenching procedure and investigated their physical and optical characteristics. Physical properties and their relationship with the composition are demonstrated. Judd-Ofelt parameters have been derived using absorption spectra of Nd^{3+} ions embedded boro-bismuth glasses and are taken to estimate radiative parameters of the fluorescent states of Nd^{3+} ions. The calculated radiative properties, experimental quantities derived from emission spectra and decay curves of the $^4F_{3/2}$ state provide comprehensive optical properties of the glasses besides their emission capability for the laser activity near 1.06 μm.

1. Introduction

Rare-earths embedded glasses are an important group of materials which find new opportunities in the fields of optical fiber amplifiers, near-infrared (NIR) laser devices, sensors, etc. [1–4]. Trivalent neodymium (Nd^{3+}) is one of the successfully used trivalent rare earth ions in the field of NIR lasers and it has also been used in glasses for halogen lamps to absorb harmful ultra-violet rays. Among the lanthanide ions, Nd^{3+} plays a vital role as it has efficient emission property in NIR region and shows marginal changes in optical properties with change in compositions [3–9].

Among different glass hosts such as oxide, germinate, fluoride, chalcogenide, etc, oxide glass is highly preferred material as a host since it is thermally and chemically stable besides transparent at the emission and excitation wavelengths [5–7,10–19]. Borate glass as a host possess several interesting properties such as easy to prepare, high viscosity, high transparency, low melting point, non-toxicity of the raw material, cheap, simplicity of preparation set up, efficient radiative transitions, homogeneity and high rare earth ions solubility. But there are only few reports on the laser action in these borate glasses and the efficiencies are also not satisfactory [4]. On the other hand, bismuth borate glasses have potential use in optoelectronic devices due to their extensive glass formation range, low melting temperature (600–800 °C), high refractive index (~2.0), non-linear optical property and high chemical and physical stability [25]. Also, RE^{3+} ions doped bismuth borate glasses are found to have higher stimulated emission cross-sections and quantum efficiencies [4,8,9,20–26]. The above properties are essential characteristics of a solid state laser gain medium.

The Nd^{3+}-doped boro-bismuth glasses, possess desirable physical and optical properties for laser applications [3,25,26]. Hence, a uniform investigation on laser spectroscopic characteristics of Nd^{3+} ions embedded boro-bismuth (BBiNd) glasses are made by varying the composition of B_2O_3 and Bi_2O_3. Judd-Ofelt (JO) parameters [27,28] were calculated using the absorption intensities of 4f-4f transitions of 1.0 mol % Nd^{3+}-doped glasses and are used to calculate radiative characteristics that include stimulated-emission cross-sections, branching ratios, transition probabilities and photoluminescence quantum efficiencies [5–26,29–38]. The results have been correlated with the experimental results of spontaneous emission and decay curves by exciting the samples with the 808 nm radiation [5–26,29–38].

Nie et al. [3], studied Bi_2O_3+B_2O_3+SiO_2 glass by fixing the Bi_2O_3 content at 43 mol % and varying B_2O_3 and SiO_2 and keeping the Nd^{3+} ions concentration at 1.0 mol %. They mainly investigated the nature of 1.3 μm emission in these glasses. The same group [9] studied

* Corresponding author.
E-mail address: ckjaya@yahoo.com (C.K. Jayasankar).

https://doi.org/10.1016/j.physb.2022.414327
Received 21 May 2022; Received in revised form 27 August 2022; Accepted 3 September 2022
Available online 8 September 2022

$70Bi_2O_3$+$20B_2O_3$+$10SiO_2$ glass system with varying Nd^{3+} content ranges from 0.1 to 1.5 mol %. In that report they studied concentration quenching effect and 1.3 μm emission properties.

Mahamuda et al. [21] investigated zinc alumino bismuth borate glasses having a composition of $60B_2O_3$+$20ZnO$+$10Al_2O_3$+(10-x) Bi_2O_3+xNd_2O_3 (where x = 0.5, 1.0, 1.5, 2.0 and 2.5 mol %) and studied their spectroscopic and luminescence properties. Karthikeyan et al. [22], prepared Nd^{3+}-doped heavy metal borate glasses of composition, $35MO$+$30Na_2O$+$34B_2O_3$+$1Nd_2O_3$ (MO = Bi_2O_3, PbO) and studied their optical and non-linear properties. They also prepared Nd^{3+}-embedded borate lead bismuth (B_2O_3 +PbO + Bi_2O_3) glasses [24] and studied their glass transition, structural and optical properties.

Chen et al. [25], made bismuth borate glasses of the compositions, (100-x) ($40Bi_2O_3$+$60B_2O_3$). xNd_2O_3 (x = 0.1, 0.3,0.5,1.0,1.5, 2.0) and studied their spectroscopic properties. Saisudha and Ramakrishna [26] prepared binary bismuth borate glasses of the composition, 97 (xBi_2O_3+(100-x)B_2O_3).$3Nd_2O_3$, x = 30, 40, 50 and 60 mol % and studied their optical absorption properties using the Judd-Ofelt theory [27,28]. Gupta et al. [36], prepared zinc-boro bismuthate glasses of the composition, (99.5-x) ($3B_2O_3$+ $4ZnO$)+xBi_2O_3+$0.5Nd_2O_3$, where x = 0, 5,10, 20, 30,40,50 and 60) and studied the role of bismuth on elastic, structural and spectroscopic characteristics.

Though optical properties of Nd^{3+} embedded boro-bismuth glasses have been reported [3,25,26], but details of experimental fluorescence properties are not at all attempted. Therefore, the present work reports detailed study of not only compositional variation of B_2O_3/Bi_2O_3, but also concentration variation of Nd^{3+} ions are systematically characterized and related both experimental results with theoretical values as well as compared with similar reported results of Nd^{3+}:glasses [3,9,21, 22,24–26,36].

2. Experimental details

Three types of Nd^{3+}-doped boro-bismuth (BnBiNd, n = 20, 50 and 70) glasses having the nomenclature, composition and dopant concentrations, prepared in the present work, are shown in Table 1 along with those of some reported boro-bismuth glasses for comparison. Glass labels for each glass composition has been framed as proposed by Chandrappa et al. [39,40]. Compositions of Nd^{3+} embedded bismuth borate glasses of the present study are listed in Table 1 along with the compositions of some reported ones [3,21,22,24–26,36].

All the glasses were prepared by melt-quenching technique. Analytical reagent grade chemicals, H_3BO_3 and Bi_2O_3 were used for host matrix while spectroscopic quality Nd_2O_3 has been used as dopant. The weight of 20 g batch mixture of raw chemicals was taken and well grinded to get a homogeneous batch. The fine mixture was taken in a crucible (alumina) for melting at 850 °C for 2 h in an electric furnace. The temperature was sufficient to produce clear and bubble free melt. The melted liquid was quickly quenched on brass mould at 300 °C and later annealed for 12 h to minimize thermal stresses produced by sudden quenching of the glass. Transparent, bubble free and homogenous glasses were obtained and taken for further characterization.

The prepared glasses are optically polished for measurement of their optical and physical characteristics. The refractive indices are estimated by Brewster's method at λ = 632 nm (diode laser). The densities are estimated using Archimedes' method with high pure distilled water for immersion. Absorption spectrum was measured on a PerkinElmer spectrophotometer (Lambda-950). The excitation, emission and decay characteristics are made with a FLS980 spectrofluorometer, where continuous and pulsed mode operation of xenon lamp has been used.

3. Results and discussion

3.1. Physical properties

All the physical properties of the BnBiNd glasses are determined using suitable expressions and are shown in Table 2. As can be seen, with increase in bismuth in the glass composition, the density also increases because of the replacement of B_2O_3 (lighter mass, mol. wt. = 61.98 gm) by Bi_2O_3 (heavier mass, mol. wt. = 465.96 gm). As can be observed, the refractive index values of the present systems increase from 1.81 to 2.24 with increase in bismuth content from 20 to 70 mol %. Similar trend of refractive index was noticed in bismuth modifier in BnBiNd (n = 29, 39, 49 and 59) [26] and BZnBiNd (n = 5,10, 20, 30,40,50 and 60) [36] glasses. The magnitude as well as variation in refractive index with variation in bismuth content are found to be comparable with those observed in BnSBiNd (n = 10,15 and 20) [3], $BBiPbNd_{1.0}$ [24], BBiNd [25], BnBiNd [26] and BZnBiNd [36] glasses. From this trend, it is

Table 1
Glass label and composition of Nd^{3+}-doped glasses of the present work (PW) and those of some reported Nd^{3+}:glasses.

S.No.	Glass label	Composition
1	$B20BiNd_{0.01}$ [PW]	$79.995H_3BO_3$+$19.995Bi_2O_3$+$0.01Nd_2O_3$
2	$B20BiNd_{0.1}$ [PW]	$79.95H_3BO_3$+$19.95Bi_2O_3$+$0.1Nd_2O_3$
3	$B20BiNd_{1.0}$ [PW]	$79.5H_3BO_3$+$19.5Bi_2O_3$+$1.0Nd_2O_3$
4	$B20BiNd_{2.0}$ [PW]	$79H_3BO_3$+$19Bi_2O_3$+$2.0Nd_2O_3$
5	$B50BiNd_{0.01}$ [PW]	$49.995H_3BO_3$+$49.995Bi_2O_3$+$0.01Nd_2O_3$
6	$B50BiNd_{0.1}$ [PW]	$49.95H_3BO_3$+$49.95Bi_2O_3$+$0.1Nd_2O_3$
7	$B50BiNd_{1.0}$ [PW]	$49.5H_3BO_3$+$49.5Bi_2O_3$+$1.0Nd_2O_3$
8	$B50BiNd_{2.0}$ [PW]	$49H_3BO_3$+$49Bi_2O_3$+$2.0Nd_2O_3$
9	$B70BiNd_{0.01}$ [PW]	$29.995H_3BO_3$+$69.995Bi_2O_3$+$0.01Nd_2O_3$
10	$B70BiNd_{0.1}$ [PW]	$29.95H_3BO_3$+$69.95Bi_2O_3$+$0.1Nd_2O_3$
11	$B70BiNd_{1.0}$ [PW]	$29.5H_3BO_3$+$69.5Bi_2O_3$+$1.0Nd_2O_3$
12	$B70BiNd_{2.0}$ [PW]	$29H_3BO_3$+$69Bi_2O_3$+$2.0Nd_2O_3$
13	$B43BiNd_{1.0}$ [3]	$57B_2O_3$+$43Bi_2O_3$+$1Nd_2O_3$
14	$B10SBiNd_{1.0}$ [3]	$47B_2O_3$+$10SiO_2$+$43Bi_2O_3$+$1Nd_2O_3$
15	$B15SBiNd_{1.0}$ [3]	$42B_2O_3$+$15SiO_2$+$43Bi_2O_3$+$1Nd_2O_3$
16	$B20SBiNd_{1.0}$ [3]	$37B_2O_3$+$20SiO_2$+$43Bi_2O_3$+$1Nd_2O_3$
17	$S20BBiNd_{1.0}$ [3]	$37.5SiO_2$+$19.5B_2O_3$+$43Bi_2O_3$+$1Nd_2O_3$
18	$S10BBiNd_{1.0}$ [3]	$47SiO_2$+$10B_2O_3$+$43Bi_2O_3$+$1Nd_2O_3$
19	$BiBSNd_{1.0}$ [9]	$70Bi_2O_3$+$25B_2O_3$+$10Si_2O_3$+$1.0Nd_2O_3$
20	$BZA9BiNd_{1.0}$ [21]	$60B_2O_3$+$20ZnO$+ $10Al_2O_3$+$9Bi_2O_3$+$1Nd_2O_3$
21	$B35BiNNd_{1.0}$ [22]	$34B_2O_3$+$35Bi_2O_3$+$30Na_2O$+$1Nd_2O_3$
22	$BBiPbNd_{1.0}$ [24]	$49B_2O_3$+$25Bi_2O_3$+$25PbO$+$1.0Nd_2O_3$
23	$B40BiNd_{0.1}$ [25]	$59.94B_2O_3$+$39.94Bi_2O_3$+$0.1Nd_2O_3$
24	$B39.9BiNd_{0.3}$ [25]	$59.82B_2O_3$+$39.88Bi_2O_3$+$0.3Nd_2O_3$
25	$B39.8BiNd_{0.5}$ [25]	$59.7B_2O_3$+$39.8Bi_2O_3$+$0.5Nd_2O_3$
26	$B39.6BiNd_{1.0}$ [25]	$59.4B_2O_3$+$39.6Bi_2O_3$+$1Nd_2O_3$
27	$B39.4BiNd_{1.5}$ [25]	$59.1B_2O_3$+$39.4Bi_2O_3$+$1.5Nd_2O_3$
28	$B39.2BiNd_{2.0}$ [25]	$58.8B_2O_3$+$39.2Bi_2O_3$+$2Nd_2O_3$
29	$B29BiNd_{1.5}$ [26]	$68.5B_2O_3$+$28.5Bi_2O_3$+$3Nd_2O_3$
30	$B39BiNd_{1.5}$ [26]	$58.5B_2O_3$+$38.5Bi_2O_3$+$3Nd_2O_3$
31	$B49BiNd_{1.5}$ [26]	$48.5B_2O_3$+$48.5Bi_2O_3$+$3Nd_2O_3$
32	$B59BiNd_{1.5}$ [26]	$38.5B_2O_3$+$58.5Bi_2O_3$+$3Nd_2O_3$
33	$BZ5BiNd_{0.5}$ [36]	$40.5B_2O_3$+$54.0ZnO$+$5Bi_2O_3$+$0.5Nd_2O_3$
34	$BZ10BiNd_{0.5}$ [36]	$38.4B_2O_3$+$51.1ZnO$+$10Bi_2O_3$+$0.5Nd_2O_3$
35	$BZ20BiNd_{0.5}$ [36]	$34.1B_2O_3$+$45.4ZnO$+$20Bi_2O_3$+$0.5Nd_2O_3$
36	$BZ30BiNd_{0.5}$ [36]	$29.8B_2O_3$+$39.7ZnO$+$30Bi_2O3$+$0.5Nd_2O_3$
37	$BZ40BiNd_{0.5}$ [36]	$25.5B_2O_3$+$34.0ZnO$+$40Bi_2O_3$+$0.5Nd_2O_3$
38	$BZ50BiNd_{0.5}$ [36]	$21.2B_2O_3$+$28.3ZnO$+$50Bi_2O_3$+$0.5Nd_2O_3$
39	$BZ60BiNd_{0.5}$ [36]	$16.9B_2O_3$+$22.6ZnO$+$60Bi_2O_3$+$0.5Nd_2O_3$

Table 2
Physical properties of the 1.0 mol % Nd^{3+} doped bismuth borate glasses.

Physical properties	$B20BiNd_{1.0}$	$B50BiNd_{1.0}$	$B70BiNd_{1.0}$
Density, d (g/cm^3)	5.11	6.83	7.53
Refractive index, n (at 632 nm)	1.81	2.01	2.24
Nd^{3+} ion concentration (N, ions/cm^3, × 10^{20})	6.03	6.32	7.43
Inter–nuclear distance, r_i (Å)	12.04	13.51	16.21
Field strength, F (× 10^{14} cm^{-2})	5.21	5.66	5.92
Molar volume, V_m (cm^3/mol)	26.31	29.21	31.12
Molar refractivity, R_m (cm^{-3})	11.61	14.30	16.24
Electric polarizability, α_e (× $10^{-22}cm^3$)	6.41	6.66	7.02
Dielectric constant (ε)	3.01	3.21	3.84
Reflection loss, R (%)	8.30	9.61	10.31
Metallization factor (M)	0.66	0.53	0.41

concluded that the higher index of refraction of the title glasses is very much favorable for making waveguide and optical fiber applications.

The inter-nuclear distance is the distance (r_i) between two nuclei of the Nd^{3+} ion in the glass matrix and can be calculated using the formula,

$$\text{Inter}-\text{nuclear distance, } r_i(A^0) = \left(\frac{1}{N}\right)^{1/3}$$

where 'N' is the concentration of Nd^{3+} ions in the glass sample.

Polaron radius is the distance from the radius of the one Nd^{3+} ion to the radius of another Nd^{3+} ion and is given by,

$$\text{Polaron radius, } r_p(A^0) = \frac{1}{2}\left(\frac{\Pi}{6N}\right)^{1/3}$$

The vector sum of all forces exerted by a field on a unit mass, unit charge, unit magnetic pole, etc., at a given point within the field is known as field strength given by,

$$\text{Field strength, } F\left(\times 10^{14}\right) cm^{-2} = \frac{Z}{(r_p)^2}$$

where 'Z' is the oxidation number of the Nd^{3+} ion.

The molar volume (V_m) of a substance is the ratio of the volume occupied by a substance to the amount of substance, usually given at a given temperature and pressure. It is equal to the molar mass (M) divided by the density (ρ), where 'M' is the effective molecular weight (sum of the products of composition and molecular weights of the chemical components of the glass material) and 'd' is the density of the glass and it is represented as,

$$\text{Molar volume, } V_m\left(cm^3/mol\right) = \frac{M}{d}$$

Molar refraction is a measure of the total polarizability of a mole of a material. Through Lorentz-Lorenz Eq., the relationship between molar refraction, R_m, refractive index (n) and molar volume (V_m) for isotropic substance such as liquid, glasses and cubic crystals can be defined as,

$$\text{Molar refractivity, } R_m\left(cm^3/mol\right) = \left(\frac{n^2-1}{n^2+1}\right) V_m$$

Electronic polarizability is the magnitude of electrons response to an electric-field which can be calculated by applying following expression,

$$\text{Electronic polarizabilty, } \alpha_e\left(10^{-22} cm^3\right) = \frac{3R_m}{4\Pi N_A}$$

The dielectric constant is the ratio of the permittivity of a substance to the permittivity of free space and is given by,

$$\text{Dielectric constant, } \varepsilon = n^2$$

The reflection loss gives the information about the reduction of intensity given by,

$$\text{Reflection loss, } R(\%) = \left(\frac{n-1}{n+1}\right)^2 \times 100$$

Metallization criterion is calculated to determine the tendency for metallization and to investigate the insulating behavior of the fabricated glasses and is given by,

$$\text{Metallization factor, } M = 1 - \frac{R_m}{V_m}$$

All the physical properties listed in Table 2, except metallization factor increases with increase in bismuth content in the glasses from $B20BiNd_{1.0}$ to $B70BiNd_{1.0}$, where as the metallization factor decreases with increase in bismuth content.

3.2. Optical absorption and Judd-Ofelt analysis

Fig. 1 presents the optical absorption spectra of 1.0 mol % Nd^{3+} ions in bismuth borate glasses. The absorption peak centers differ slightly with change in glass compositions. The observed absorption peaks are the consequence of exciting the ground multiplet ($^4I_{9/2}$) of Nd^{3+} ions in glass matrices to the excited states [11,18,20,34,40–43]. There are 9, 8 and 7 absorption bands for the $B20BiNd_{1.0}$, $B50BiNd_{1.0}$ and $B70BiNd_{1.0}$ glass systems, respectively. The observed peak energies of the Nd^{3+}-doped boro-bismuth glasses are given in Table 3. Areas under the respective absorption bands are used to calculate the experimental oscillator strengths (f_{exp}) using the following Eq.,

$$f_{\exp} = \frac{2.303mc^2}{N\pi e^2}\int \varepsilon(\upsilon)d\upsilon = 4.318\times 10^{-9}\int \varepsilon(\upsilon)d\upsilon \quad (1)$$

From Judd-Ofelt analysis, the calculated oscillator strength (f_{cal}) is given as,

$$f_{cal} = \frac{8\pi^2 mc\upsilon}{3h(2J+1)}\frac{(n^2+2)^2}{9n}\sum_{\lambda=2,4,6}\Omega_\lambda\left(\psi J||U^\lambda||\psi' J'\right)^2 \quad (2)$$

here 'm' represents the mass of the electron, 'c' indicates light velocity, 'n' is the refractive index, 'ν' corresponds the transition energy (cm^{-1}), 'h' represents the Plank's constant, $(n^2+2)^2/9n$ indicates Lorentz local field correction of the absorption state, 'J' corresponds the angular momentum of the ground level, $\Omega_{\lambda,}$ ($\lambda = 2$, 4 and 6) are the phenomenologically fitted JO intensity parameters and $||U^{(\lambda)}||^2$ are the matrix elements of the rank $\lambda = 2$, 4 and 6 and are evaluated through intermediate coupling for the ψJ → ψ'J' transition. These matrix elements are independent of host. By applying standard Judd-Ofelt theory on distinct energy levels of Nd^{3+} ions in bismuth borate glasses, theoretical (calculated) oscillator strengths are estimated using least squares fit approach using Eq. (2) and the reduced matrix elements reported elsewhere [44].

Table 3 presents the energy position of the absorption bands, their experimental and theoretical oscillator strengths along with JO parameters, spectroscopic quality factor and root mean square (rms) deviation for BnBiNd glasses. The rms values between f_{exp} and f_{cal} are ±0.36, ±0.43 and ±0.81 for $B20BiNd_{1.0}$, $B50BiNd_{1.0}$ and $B70BiNd_{1.0}$ glasses, respectively. The rms deviation between calculated and experimental oscillator strengths is considerably less for all the glasses, suggesting the accuracy of JO analysis. The intensities of some 4f-4f transitions are higher compared to other transitions which are identified by the larger quantities of matrix element $(\psi J||U^2||\psi' J')^2$ [44].

The Judd-Ofelt intensity parametrization is highly beneficial to

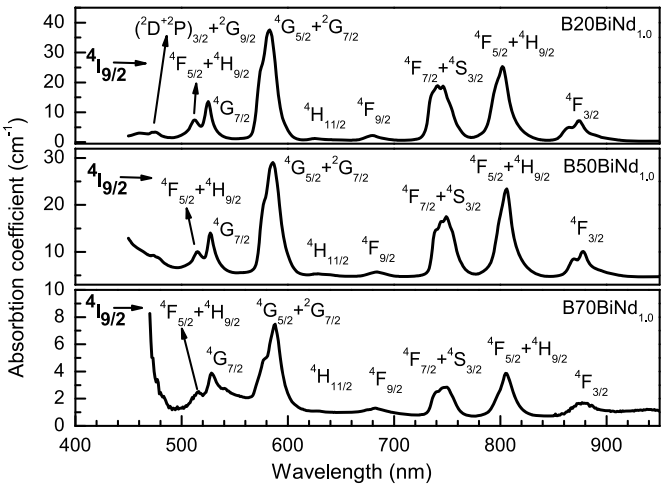

Fig. 1. Absorption spectra of BnBiNd glasses in the UV–Visible–NIR region.

Table 3
Optical absorption transitions with peak positions, experimental (f_{exp}) and calculated (f_{cal}) oscillator strengths (x10^{-6}), rms deviations (σ_{rms}), JO intensity parameters (Ω_λ, (λ = 2,4,6), × 10^{-20} cm^2) and spectroscopic quality factors (Ω_4/Ω_6) of 1.0 mol % Nd^{3+} ions-doped $BnBiNd_{1.0}$ glasses.

Transition $^4I_{9/2}$ →	$B20BiNd_{1.0}$			$B50BiNd_{1.0}$			$B70BiNd_{1.0}$		
	Energy (nm)	f_{exp}	f_{cal}	Energy (nm)	f_{exp}	f_{Cal}	Energy (nm)	f_{exp}	f_{Cal}
$^4F_{3/2}$	874	3.24	3.27	878	2.24	2.47	878	1.35	2.24
$^4F_{5/2} + {}^4H_{9/2}$	801	10.35	9.86	805	9.35	8.63	807	8.32	6.89
$^4F_{7/2} + {}^4S_{3/2}$	741	9.89	10.27	749	8.89	9.43	749	6.03	7.101
$^4F_{9/2}$	679	0.64	0.42	683	0.99	0.72	681	0.45	0.557
$^4H_{11/2}$	625	0.27	0.222	627	0.34	0.200	626	0.15	0.155
$^4G_{5/2} + {}^2G_{7/2}$	582	19.09	19.06	585	14.06	14.05	587	9.09	9.02
$^4G_{7/2}$	525	4.24	4.60	527	3.24	3.63	528	2.35	3.16
$^4G_{9/2} + {}^2K_{13/2}$	512	2.48	2.83	514	2.65	3.25	–	–	–
$(^2D+{}^2P)_{3/2} + {}^2G_{9/2}$	475	3.65	4.21	–	–	–	–	–	–
σ_{rms}		±0.36			±0.43			±0.81	
Ω_2		4.30			2.24			0.94	
Ω_4		4.67			3.96			2.63	
Ω_6		5.99			4.81			2.78	
Ω_4/Ω_6		0.77			0.86			0.94	

predict required radiative characteristics of rare earths embedded in any glass host. From the JO parameter quantities shown in Table 3, it is observed that the order of the JO parameters for all the three $BnBiNd_{1.0}$ glasses is $\Omega_6 > \Omega_4 > \Omega_2$. The parameter, Ω_2 mainly influences the site asymmetry of Nd^{3+} and also the covalence bonding of Nd^{3+}-O^{2-}. The Bi^{3+} possesses lower field strength than B^{3+} and hence exhibit strong ionic bond with O^{2-} ligands anions. This results in comparatively higher covalent bonding of Ln^{3+} active ions with O^{2-}, which could be a reason for the noted decrease in Ω_2 magnitudes for glasses with higher Bi_2O_3.

Even though, Ω_4 and Ω_6 values do not reveal any role on nature of environment structure, they together show considerable influence on radiative properties of luminescence transitions originating from the $^4F_{3/2}$ level to its lower multiplets, $^4I_{15/2}$, $^4I_{13/2}$ and $^4I_{9/2}$. This occurs mainly because in the case of Nd^{3+}, as the matrix element of $(\psi J||U^2||\psi' J')^2 = 0$ [44] for transitions originating from $^4F_{3/2}$ excited level to lower multiplets ($^4I_{15/2}$, $^4I_{13/2}$ and $^4I_{9/2}$) and hence the value of $\Omega_4/\Omega_6 = \chi$, defined as the spectroscopic quality factor. The 'χ' values of the $BnBiNd_{1.0}$ glasses are presented in Table 3. Lesser value of 'χ' favors the lasing action for $^4F_{3/2} \rightarrow {}^4I_{11/2}$ transition over $^4F_{3/2} \rightarrow {}^4I_{9/2}$ and vice versa. If the quality factor increases, the fluorescence efficiency also increases. In the present study, it is found that the quality factor varies directly with the bismuth content in the composition.

3.3. Radiative properties and emission spectra

Fig. 2 shows the partial electronic energy level diagram of Nd^{3+} ions indicating the excitation and possible NIR emission channels of BnBiNd glasses along with cross-relaxation (CR) and non-radiative (NR) channels. The emission spectra are measured for all the glasses of the present study, exciting with 808 nm and monitoring the emission between 850 and 1450 nm which are presented in Fig. 3.

The radiative emission spectra of all the glasses exhibit three emission bands corresponding to $^4F_{3/2} \rightarrow {}^4I_{9/2}$, $^4I_{11/2}$ and $^4I_{13/2}$ transitions around 905, 1065 and 1340 nm, respectively. In these three bands, the $^4F_{3/2} \rightarrow {}^4I_{11/2}$ (1065 nm) is found to be the most intense and $^4F_{3/2} \rightarrow {}^4I_{13/2}$ (1339 nm) is found to be weak intensity in all the glasses. The intensity of $^4F_{3/2} \rightarrow {}^4I_{11/2}$ band increases with increase in Nd^{3+} ions concentration and quenching has been observed after 1.0 mol % of Nd^{3+} ions . This quenching is due to the energy transfer process through cross-relaxation process ($^4F_{3/2}$: $^4I_{9/2} \rightarrow {}^4I_{15/2}$: $^4I_{15/2}$) as depicted in Fig. 3 [11, 18,20,34,40–42]. It can be noted from Fig. 3 that the relative intensity value of $^4F_{3/2} \rightarrow {}^4I_{11/2}$ emission has become more preferable with respect to $^4F_{3/2} \rightarrow {}^4I_{9/2}$ transitions with the increase in bismuth content which is also evident from the Ω_4/Ω_6 magnitudes, estimated from JO parameters. Luminescence properties of Nd^{3+} ions increase with increase in Bi_2O_3 content leading to improved radiative properties [36].

For treating the emission process, electric (A_{ed}) and magnetic (A_{md})

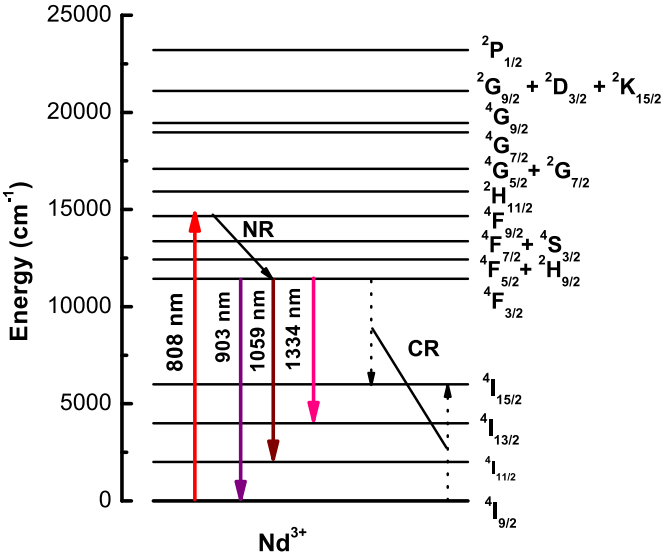

Fig. 2. Partial energy level diagram of the Nd^{3+} ions in BnBiNd glasses showing the possible near-infrared emission transitions along with non-radiative (NR) and cross-relaxation (CR) channels.

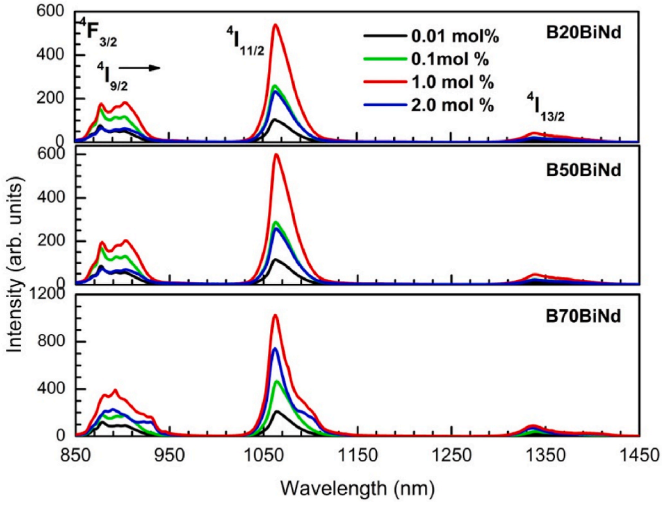

Fig. 3. Near-infrared emission spectra (λ_{ex} = 808 nm) of the BnBiNd glasses for different concentrations of Nd^{3+} ions.

dipole radiative transition probabilities have been evaluated by the following expressions [11,18,20,34,40–42].

$$A_{ed}(\psi J,\psi' J') = \frac{64\pi^4\nu^3}{3h\ (2J+1)}\ \frac{n\ (n^2+2)^2}{9} S_{ed}(\psi J,\psi' J') \quad (3)$$

$$A_{md}(\psi J,\psi' J') = \frac{64\pi^4\nu^3}{3h\ (2J+1)}\ n^3 S_{md}(\psi J,\psi' J') \quad (4)$$

Total of the A_{ed} and A_{md} gives the radiative transition probability (A_R) for a given transition as

$$A_R(\psi J,\psi' J') = A_{ed}(\psi J,\psi' J') + A_{md}(\psi J,\psi' J') \quad (5)$$

$$A_R(\psi J,\psi' J') = \frac{64\pi^4\nu^3}{3h\ (2J+1)}\left[\frac{n\ (n^2+2)^2}{9} S_{ed} + n^3 S_{md}\right] \quad (6)$$

The total transition probability of fluorescent level is the sum of the radiative transition probabilities of all lower terminal levels,

$$A_T(\psi J) = \sum_{\psi' J'} A_R\ (\psi J,\ \psi' J') \quad (7)$$

The radiative lifetime (τ_R) of an excited level estimated to be from the total radiative transition rate (A_T) by the following relation,

$$\frac{1}{\tau_R} = A_T(\psi J) = \sum_{\psi' J'} A_R\ (\psi J,\ \psi' J') \quad (8)$$

The electrons in an excited state are relaxed to several lower energy states, the calculated branching ratio (β_R) can be obtained by the following expression,

$$\beta_R\left(\psi J,\psi' J'\right) = \frac{A_R(\psi J,\psi' J')}{A_T(\psi J)} \quad (9)$$

These β_R could be taken to evaluate the intensities of all emission transitions coming from an excited fluorescent level. The experimental β_R (β_{exp}) can be evaluated using the relative areas of the emission levels. The β_R is an important quantity for the designing of laser gain media, as it indicates possibility of achieving stimulated emission for a given emission channel.

The most important characteristic property that controls the laser performance of a laser material is nothing but stimulated emission cross-section ($\sigma(\lambda_p)$) which can be calculated using the emission spectra through the expression,

$$\sigma_e(\psi J,\psi' J') = \frac{\lambda_p^4}{8\pi c n^2 \Delta\lambda_{eff}} A_R(\psi J,\psi' J') \quad (10)$$

here λ_P denotes the emission peak in nm, $\Delta\lambda_{eff}$ corresponds effective linewidth of the emission band (nm) which is also known as fullwidth at half maximum (FWHM) of the emission level estimated by taking ratio of the area of the emission level and its average height.

Tables 4–6 present the radiative properties like emission peak positions (λ_p), β_{exp}, β_{cal}, A_R, $\Delta\lambda_{eff}$, $\sigma(\lambda_p)$ and gain bandwidth which is the product of $\Delta\lambda_{eff} \times \sigma(\lambda_p)$ for the emission transitions, $^4F_{3/2} \rightarrow {}^4I_J$ (J = 15/2, 13/2, 11/2and 9/2) and lifetime (τ_R) of the $^4F_{3/2}$ state for $B20BiNd_{1.0}$, $B50BiNd_{1.0}$ and $B70BiNd_{1.0}$ glasses, respectively, derived using JO intensity parameters and emission spectra [11,18,20,34,40–42].

From Tables 4–6, τ_R values for $^4F_{3/2} \rightarrow {}^4I_{11/2}$ emission channel are calculated to be 182, 163 and 153 μs whereas $\sigma(\lambda_p)$ values are found to be 2.97, 4.0 and 3.15 × 10^{-20} cm^2 for $B20BiNd_{1.0}$, $B50BiNd_{1.0}$ and $B70BiNd_{1.0}$, glasses, respectively. As can be seen, radiative lifetimes of the $B20BiNd_{1.0}$ glass has higher value while emission cross-section of the $B50BiNd_{1.0}$ glass has higher value among the three glasses. The experimental decay curves and further analysis of relaxation or energy transfer mechanisms should give an insight into the performance of the glasses.

Table 4
Emission peak positions (λ_p, nm), experimental (β_{exp}) and calculated (β_{cal}) branching ratios, radiative transition probabilities (A_R, s^{-1}), effective bandwidths ($\Delta\lambda_{eff}$, nm), stimulated emission cross-sections ($\sigma(\lambda_p)$, × 10^{-20}, cm^2) and radiative lifetime (τ_R, μs), gain bandwidth ($\Delta\lambda_{eff} \times \sigma(\lambda_p)$, × 10^{-28} cm^3) of NIR emission transitions of $B20BiNd_{1.0}$.

Transition $^4F_{3/2} \rightarrow$	λ_p (nm)	Branching ratios		A_R	$\Delta\lambda_{eff}$	$\sigma(\lambda_p)$	$\Delta\lambda_{eff} \times \sigma(\lambda_p)$
		β_{exp}	β_{cal}				
$^4I_{13/2}$	1339	0.14	0.11	560	28	1.67	47
$^4I_{11/2}$	1064	0.60	0.50	2749	31	2.97	92
$^4I_{9/2}$	904	0.36	0.39	2128	48	0.69	33
				A_T = 5465			
				τ_R = 182			

Table 5
Emission peak positions (λ_p, nm), experimental (β_{exp}) and calculated (β_{cal}) branching ratios, radiative transition probabilities (A_R, s^{-1}), effective bandwidths ($\Delta\lambda_{eff}$, nm), stimulated emission cross-sections ($\sigma(\lambda_p)$, × 10^{-20}, cm^2) and radiative lifetime (τ_R, μs), gain bandwidth ($\Delta\lambda_{eff} \times \sigma(\lambda_p)$, × 10^{-28} cm^3) of NIR emission transitions of $B50BiNd_{1.0}$.

Transition $^4F_{3/2} \rightarrow$	λ_p (nm)	Branching ratios		A_R	$\Delta\lambda_{eff}$	$\sigma(\lambda_p)$	$\Delta\lambda_{eff} \times \sigma(\lambda_p)$
		β_{exp}	β_{cal}				
$^4I_{13/2}$	1304	0.07	0.10	655	45	1.32	59
$^4I_{11/2}$	1063	0.57	0.50	3246	29	4.00	116
$^4I_{9/2}$	904	0.36	0.40	2577	48	0.91	43
				A_T = 6510			
				τ_R = 163			

Table 6
Emission peak positions (λ_p, nm), experimental (β_{exp}) and calculated (β_{cal}) branching ratios, radiative transition probabilities (A_R, s^{-1}), effective bandwidths ($\Delta\lambda_{eff}$, nm), stimulated emission cross-sections ($\sigma(\lambda_p)$, × 10^{-20}, cm^2) and radiative lifetime (τ_R, μs), gain bandwidth ($\Delta\lambda_{eff} \times \sigma(\lambda_p)$, × 10^{-28} cm^3) of NIR emission transitions of $B70BiNd_{1.0}$.

Transition $^4F_{3/2} \rightarrow$	λ_p (nm)	Branching ratios		A_R	$\Delta\lambda_{eff}$	$\sigma(\lambda_p)$	$\Delta\lambda_{eff} \times \sigma(\lambda_p)$
		β_{exp}	β_{cal}				
$^4I_{13/2}$	1341	0.05	0.10	569	28	1.69	47
$^4I_{11/2}$	1064	0.6	0.48	2921	31	3.15	98
$^4I_{9/2}$	903	0.35	0.42	2511	48	0.81	39
				A_T = 6748			
				τ_R = 153			

For efficient optical systems, the gain bandwidth parameter ($\Delta\lambda_{eff} \times \sigma(\lambda_p)$, × 10^{-28} cm^3) should be as high as possible to attain high gain and in the present glasses the gain bandwidth values have been calculated and are shown in Tables 4–6 for $B20BiNd_{1.0}$, $B50BiNd_{1.0}$ and $B70BiNd_{1.0}$ glasses, respectively. The values are found to be comparable with those of reported Nd^{3+}-doped glasses [6,34,36,42] and are lower than those of $SLBNd_{1.0}$ [6] glasses.

3.4. Decay curve analysis

The lifetime is also an important characteristic parameter to analyse laser gain medium. Fig. 4 shows the decay curves of $^4F_{3/2}$ level measured by exciting at 808 nm and monitoring the emission at 1065 nm. For all the three sets of glass samples, it is observed that the decay curve shows

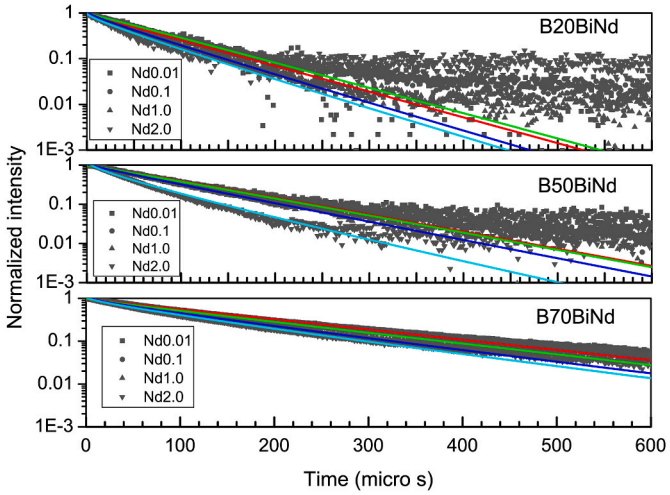

Fig. 4. Decay curves for the $^4F_{3/2}$ level in BnBiNd glasses for different concentrations of Nd^{3+} ions under 808 nm excitation (solid line represents the I–H model fitting).

nearly mono-exponential trend for lower concentrations and tend to transform into bi-exponential at higher active ion concentrations.

Many transitions and larger emission probabilities from initial level causes to quick decay resulting in very short lifetimes. The calculated lifetime (τ_R) via JO parameters are compared to the experimental lifetimes (τ_{mes}). The difference between τ_R and τ_{mes} arises due to the presence of multiphonon non-radiative relaxation processes as given by,

$$W_{NR} = \frac{1}{\tau_{mes}} - \frac{1}{\tau_R} \tag{11}$$

where W_{NR} refers the non-radiative transition probability (s^{-1}), τ_R corresponds to radiative lifetime and τ_{mes} refers the experimental lifetime. Using τ_{mes} and τ_R, quantum efficiency (η) can be calculated as,

$$\eta = \frac{\tau_{mes}}{\tau_R} \tag{12}$$

In the present glasses, only Nd^{3+} ion is the active ion. Hence, both acceptor and donor ions are Nd^{3+} ions only. In the presence of acceptor ions, donor in the vicinity of acceptors can interact among them through multipolar or exchange forces and can transfer energy. The rate of transfer for different acceptor-donor pairs depend quite significantly with the strength of the acceptor-donor interaction and normally decreases quickly on par their separation. With the increase in concentration, the distance between the ions is sufficiently small enough that the ions can interact greatly. These processes are found to be due to either the interaction between similar or/and different dopant ions.

The interaction between the active ions can be due to different magnetic and electric multipolar interactions between adjacent Nd^{3+} ions. These interaction processes were investigated by Dexter [45] and Förster [46] for energy transfer in complexes involving electric dipole-dipole interaction. The work by Dexter [45] and Kushida [47] have taken the contribution of electric dipole-quadrupole, electric dipole-dipole, and exchange interactions and obtained relation for the luminescence yield for different concentrations of active ions. Inokuti and Hirayama [48] revised the theory and considered energy transfer between intra 4f – 4f levels of triply ionized lanthanide ions and concluded that the luminescence decay can be explained by the following Eq.,

$$I(t) = I_0 \exp\left\{ -\frac{t}{\tau_0} - Q\left(\frac{t}{\tau_0}\right)^{3/S} \right\} \tag{13}$$

where 't' corresponds the time after excitation, τ_0 represents donors intrinsic decay time when there are no acceptors and 'Q' is the energy transfer parameter given by,

$$Q = \frac{4\pi}{3}\Gamma\left(1 - \frac{3}{S}\right) N_A R_0^3 \tag{14}$$

The value of 'Q' depends on $\Gamma(x)$ (gamma function) which in turn depends on 'S'. If S = 6, then $\Gamma(x) = 1.77$ which refers dipole-dipole; if S = 8, then $\Gamma(x) = 1.43$ corresponds to dipole-quadrupole and S = 10, then $\Gamma(x) = 1.3$ belongs to quadrupole-quadrupole interactions. N_A indicates the concentration of acceptors, which is more or less same as that of total Ln^{3+} concentration and R_0 refers the critical transfer distance which is equal to acceptor-donor separation for which energy transfer rate between acceptor and donor is same as intrinsic decay rate, τ_0^{-1}. The dipole-dipole interaction value (C_{DA}) is co-related to R_0 as,

$$C_{DA} = \frac{R_0^{(S)}}{\tau_0} \tag{15}$$

The values of measured lifetimes, quantum efficiencies, non-radiative relaxation rates, acceptor-donor interaction, critical transfer distances and energy transfer parameters for 0.01, 0.1, 1.0 and 2.0 mol % of Nd^{3+} in the present glasses are presented in Table 7. It could be inferred that all the non-exponential decay curves relatively have good fit to S = 6. It is also noticed that as the concentration of Nd^{3+} ions increases, τ_{exp} of the $^4F_{3/2}$ level decreases and the non-radiative relaxation rate increases due to energy transfer between Nd^{3+} via cross-relaxation ($^4F_{3/2}$,$^4I_{9/2}$ → $^4I_{15/2}$,$^4I_{15/2}$) which is also responsible for the quenching of emission at higher concentrations. Similarly, the values of C_{DA}, 'Q' and R_0 increases with Nd^{3+} ions concentration in all the sets of glasses as presented in Table 7. Among the glasses studied, $B70BiNd_{1.0}$ glass is found to be a very good candidate for the laser performance as it has highest measured lifetime of 123 μs and an efficiency of 80%.

For efficient laser action, the figure of merit ($\sigma(\lambda_p) \times \tau_{mes,} \times 10^{-20}$ cm^2 μs) should be as large as possible to attain high-gain. In the present study, the figure of merit (FOM) has been calculated to be 172 for B20BiNd, 324 for B50BiNd and 387 for B70BiNd glasses and are shown in Table 7. The magnitude of FOM for the present glass is lower compared to $BSLBNd_{1.0}$ [34] and $PKSAFNd_{1.0}$ [42] and are comparable to those of $ZnBBiNd_{1.0}$ [36] and $SLBNd_{1.0}$ [6] glasses. The present analysis suggests that the Nd^{3+}-doped bismuth borate glasses can be a suitable host for lasing emission at 1064 nm and also for optical amplification applications.

Table 8 presents glass labels, concentration of Nd^{3+} ions, densities, refractive indices, JO parameters, total radiative transition probabilities,

Table 7
Measured lifetimes (τ_{exp}), quantum efficiencies (η %), non-radiative relaxation rates (W_{nr}, s^{-1}), energy transfer parameters (Q), critical donor-acceptor transfer distances (R_0, A^0), dipole-dipole interaction parameters (C_{DA}, x10-^{42}), for different concentrations of Nd^{3+} ions and figure of merit (FOM, $\sigma(\lambda_p) \times \tau_{mes,} \times 10^{-20}$ cm^2 μs) of the $^4F_{3/2}$ → $^4I_{11/2}$ transition for 1.0 mol% of Nd^{3+} ions in different sets of bismuth-bortate glasses.

Glass set	Nd^{3+} concentration	τ_{mes}	η	W_{nr}	Q	R_0	C_{DA}
B20BiNd	0.01	77	–	–	–	–	–
	0.1	75	–	–	0.09	4.66	2.54
	1	58	32	10297	0.35	4.27	42.3
	2	37	–	–	0.45	2.67	71.2
FOM = 172							
B50BiNd	0.01	97	–	8016	–	–	–
	0.1	91	–	8695	0.09	5.68	0.82
	1	81	50	10052	0.17	3.30	2.96
	2	50	–	17706	0.86	2.67	77.3
FOM = 324							
B70BiNd	0.01	180	–	1906	–	–	–
	0.1	161	–	2562	0.13	4.70	3.21
	1	123	80	4480	0.42	4.26	32.6
	2	117	–	4897	0.57	2.89	58.9
FOM = 387							

Table 8
Glass labels, concentrations (C, x10^{22} cm^{-3}) of Nd^{3+} ions, densities (g, cm^{-3}), refractive indices (RI), JO parameters (Ω_λ, $\lambda = 2,4,6 \times 10^{-20}$ cm^2), total radiative transition probabilities (A_T, s^{-1}), calculated (τ_R) and experimental (τ_{exp}) lifetimes (μs) and quantum efficiencies (QE, %) of the $^4F_{3/2}$ level in $BnBiNd_{1.0}$ glasses and those of reported Nd^{3+}-doped glasses.

S.No.	Glass label	C	g	RI	Ω_2	Ω_4	Ω_6	A_T	τ_R	τ_{exp}	QE
1	$B20BiNd_{1.0}$ [PW]	603	5.11	1.810	4.30	4.67	5.99	5465	182	58	32
2	$B50BiNd_{1.0}$ [PW]	632	6.83	2.010	2.24	3.96	4.81	6510	163	81	50
3	$B70BiNd_{1.0}$ [PW]	743	7.53	2.240	0.94	2.63	2.78	6748	153	123	80
4	$B43BiNd_{1.0}$ [3]	2.89	5.78	1.952	4.03	3.00	3.31		411	288	70
5	$B10SBiNd_{1.0}$ [3]	2.94	5.87	1.953	4.09	2.57	3.65		414	297	72
6	$B15SBiNd_{1.0}$ [3]	2.96	5.88	1.956	4.16	2.98	3.61		391	313	80
7	$B20SBiNd_{1.0}$ [3]	3.00	5.96	1.973	4.04	2.73	3.60		393	298	76
8	$S20BBiNd_{1.0}$ [3]	3.04	5.99	1.973	4.40	3.35	3.79		365	318	87
9	$S10BBiNd_{1.0}$ [3]	3.07	6.04	1.978	4.31	3.03	3.73		368	332	90
10	$S43BiNd_{1.0}$ [3]	3.15	6.16	1.993	4.49	3.13	3.53		355	343	97
11	$BiBSNd_{1.0}$ [9]	25.4	7.27	2.180	4.42	3.06	3.26		412	317	77
12	$BZA9BiNd_{1.0}$ [21]		3.29	1.805	5.31	3.84	4.61	4301	232	–	–
13	$B35BiNNd_{1.0}$ [22]	7.00	4.90	1.800	4.72	2.12	3.93	2862	349		
14	$BBiPbNd_{1.0}$ [24]	1.66	5.78	1.851	1.58	4.48	3.33				
15	$B40BiNd_{0.1}$ [25]	33.0		2.000	3.71	2.59	4.24		206	84	41
16	$B39.9BiNd_{0.3}$ [25]	100		2.000	3.80	3.77	4.59		170	86	51
17	$B39.8BiNd_{0.5}$ [25]	166		2.000	3.28	3.88	4.24		176	95	54
18	$B39.6BiNd_{1.0}$ [25]	324		2.000	3.22	3.84	4.33		175	71	41
19	$B39.4BiNd_{1.5}$ [25]	501		2.000	2.70	4.10	4.47		167	54	32
20	$B39.2BiNd_{2.0}$ [25]	644		2.000	2.61	3.86	4.24		177	45	25
21	$B29BiNd_{1.5}$ [26]	1003	5.51	1.920	4.65	2.90	5.85				
22	$B39BiNd_{1.5}$ [26]	948	6.26	2.030	4.29	3.00	6.02				
23	$B49BiNd_{1.5}$ [26]	916	7.40	2.130	4.24	3.31	6.12				
24	$B59BiNd_{1.5}$ [26]	866	7.61	2.210	4.12	3.30	6.06				
25	$B57ZNd_{0.5}$ [36]	282	3.64	1.661	3.45	3.61	4.36	2766	361	58	16
26	$BZ5BiNd_{0.5}$ [36]	266	4.41	1.773	3.56	4.30	4.87	3910	256	67	26
27	$BZ30BiNd_{0.5}$ [36]	197	6.45	2.021	2.80	4.53	4.49	5920	169	83	49
28	$BZ60BiNd_{0.5}$ [36]	154	7.97	2.299	2.42	3.76	3.45	7633	131	96	73

quantum efficiencies, calculated and experimental lifetimes of $^4F_{3/2}$ level in the present study along with similar parameters of some reported Nd^{3+}-doped bismuth borate glasses [3,9,21,22,24–26,36]. Of all the glasses that are shown in Table 8, the $B29BiNd_{1.5}$ [26] has highest and $BBiPbNd_{1.0}$ [24] has the lowest concentration of Nd^{3+} ions. Density is found to be highest for the $BZ60BiNd_{0.5}$ glass [36] and lowest for the $BZA9BiNd_{1.0}$ glass [21]. Refractive index is highest for the $B70BiNd_{1.0}$ glass and is lowest for the $B57ZNd_{0.5}$ glass [36].

Of all the glasses that are compared in Table 8, the Ω_λ parameters are highest for $B20BiNd_{1.0}$ glass and Ω_2 and Ω_6 are lowest for the $B70BiNd_{1.0}$ glass. The Ω_λ values of other glasses are intermediate between these values. Calculated lifetimes are highest for the $B10SBiNd_{1.0}$ glass [3] and lowest for $BZ60BiNd_{0.5}$ glass [36] whereas experimental lifetimes are highest for $S43BiNd_{1.0}$ [3] glass and lowest for the $B39.2BiNd_{2.0}$ glass [25]. Quantum efficiencies are found to be highest for the $S43BiNd_{1.0}$ glass [3] and lowest for the $B57ZNd_{0.5}$ glass [36]. Further, uniform investigations are necessary to explain the non-uniform variations of the above parameters in the glass systems presented in Table 8.

4. Conclusions

Three compositions of boro-bismuth glasses embedded various concentrations (0.01–2.0 mol %) of Nd^{3+} ions have been prepared by melt quenching method. The optical properties of the glasses are analyzed through UV–visible–NIR absorption and photo luminescence spectra and lifetime measurements. The Judd-Ofelt intensity parameters are evaluated from the absorption transition intensities of Nd^{3+} (1.0 mol %) embedded glasses and are used to determine the radiative properties for the excited fluorescent states of Nd^{3+}:BnBiNd glasses. The $^4F_{3/2} \rightarrow {}^4I_{11/2}$ transition is having higher stimulated emission cross-section, branching ratio and radiative transition probability. The decays of $^4F_{3/2}$ (Nd^{3+}) are single exponential in nature for lower concentrations and as the concentration of the dopant ions increases, the decay curves transform to non-exponential nature. Inokuti and Hirayama model has been used to determine the energy transfer parameters, critical transfer distances and dipole-dipole interaction parameters. The analyzed optical properties indicate that $B70BiNd_{1.0}$ is the optimum glass composition for laser applications.

Credit author statement

All authors listed have made a significant contribution to the research reported in the present manuscript and have Writing - original draft, Conceptualization, read, review, editing and supervision. Furthermore, all those who made substantive contributions to this work have been included in the author list. K. Udaya Kumar, P. Babu, Ch. Basavapoornima, R. Praveena, Shobha Rani Depuru: Conceptualization, Methodology, Software, Formal analysis, Data curation, Writing Original draft preparation, Editing. C.K. Jayasankar: Investigation, Supervision, Reviewing.

Declaration of competing interest

The authors declare that they have no known competing financial interests or personal relationships that could have appeared to influence the work reported in this paper.

Data availability

Data will be made available on request.

Acknowledgements

The author (CKJ) is highly indebted to DAE-BRNS, Mumbai (No.2009/34/36/BRNS/3174, dt.12-02-2010) for the financial support under MoU research project and also to UGC, New Delhi, India (No. F.18–1/2011/(BSR), dt.24-11-2017) for awarding UGC-BSR Faculty Fellow.

References

[1] P.D. Dragic, M. Cavillon, J. Ballato, Materials for optical fiber lasers: a review, Appl. Phys. Rev. 5 (2018), 041301.

[2] J.H. Campbell, T.I. Suratwala, Nd-doped phosphate glasses for high-energy/high peak-power lasers, J. Non-Cryst. Solids 263&264 (2000) 318–341.
[3] Q. Nie, X. Li, S. Dai, T. Xu, Y. Chen, X. Zhang, Investigation of 1.3 micron emission in Nd^{3+}-doped bismuth-based oxide glasses, Physica B 400 (2007) 88–92.
[4] Y.J. Chen, X.H. Gong, Y.F. Lin, Z.D. Luo, Y.D. Huang, Quasi-continuous-wave 1065 nm laser oscillation in Nd^{3+}-doped bismuth borate glasses, Opt. Mater. 33 (2010) 71–74.
[5] O. Soriano-Romero, M.Y. Espinosa-Ceron, S. Carmona-T′ellez, A. Lira, U. Caldino, R. Lozada-Morales, A.N. Meza-Rocha, Spectroscopic analysis of Nd^{3+}-doped cadmium-vanadate invert glasses for near-infrared laser applications, J. Non-Cryst. Solids 572 (2021), 121085.
[6] F. Zaman, G. Rooh, N. Srisittipokakun, S. Ruengsri, H.J. Kim, J. Kaewkhao, Luminescence behavior of Nd^{3+}-activated soda-lime-borate glasses for solid-state lasers applications, J. Non-Cryst. Solids 452 (2016) 307–311.
[7] M. Djamal, L. Yuliantini, R. Hidayat, N. Rauf, M. Horprathum, R. Rajaramakrishna, K. Boonin, P. Yasaka, J. Kaewkhao, V. Venkatramu, S. Kothan, Spectroscopic study of Nd^{3+} ion-doped Zn-Al-Ba borate glasses for NIR emitting device applications, Opt. Mater. 107 (2020), 110018.
[8] C. Tian, Xi Chen, Y. Shuibao, Concentration dependence of spectroscopic properties and energy transfer analysis in Nd^{3+}-doped bismuth silicate glasses, Solid State Sci. 48 (2015) 171–176.
[9] Q. Nie, X. Li, S. Dai, T. Xu, Z. Jin, X. Zhang, Investigation of concentration quenching and 1.3 μm emission in Nd^{3+}-doped bismuth glasses, Spectrochim. Acta A 70 (2008) 537–541.
[10] T. Srikumar, M.G. Brik, Ch Srinivasa Rao, Y. Gandhi, D.K. Rao, V. Ravi Kumar, N. Veeraiah, Spectral and fluorescent kinetics features of Nd^{3+} ion in Nb_2O_5, Ta_2O_5 and La_2O_3 mixed lithium zirconium siicate glasses, Spectrochim. Acta 81 (2011) 498–503.
[11] M. Sundara Rao, V. Sudarsan, M.G. Brik, K. Bhargavi, Ch SrinivasRao, Y. Gandhi, N. Veeraiah, The de-clustering influence of aluminum ions on the emission features of Nd^{3+} ions in PbO-SiO_2 glasses, Opt Commun. 298–299 (2013) 135–140.
[12] S. Mohan, K.S. Thind, Investigation of luminescence and spectroscopic properties of Nd^{3+} ions in cadmium alkali borate glasses, Opt. Mater. 57 (2016) 134–139.
[13] G.V. Vazquez, G.H. Munoz, I. Camarillo, C. Falcony, U. Caldino, A. Lira, Spectroscopic analysis of a novel Nd^{3+} activated barium borate glass for broadband laser amplification, Opt. Mater. 46 (2015) 97–103.
[14] S. Mohan, K.S. Thind, Optical and spectroscopic properties of neodymium doped cadmium-sodium borate glasses, Opt Laser. Technol. 95 (2017) 36–41.
[15] K. Srinivasa Rao, Valluri Ravi Kumar, Y. Zhydachevskii, A. Suchocki, M. Piasecki, Y. Gandhi, V. Ravi Kumar, N. Veeraiah, Luminescence emission features of Nd^{3+} ions in PbO-Sb_2O_3 glasses mixed with Sc_2O_3/Y_2O_3/HfO_2, Opt. Mater. 69 (2017) 181–189.
[16] G.A. Kumar, E. De la Rosa-Cruz, K. Ueda, A. Martinez, O. Barbosa-Garcia, Enhancement of optical properties of Nd^{3+} doped fluorophosphate glasses by alkali and alkaline earth metal co-doping, Opt. Mater. 22 (2003) 201–213.
[17] B. Karthikeyan, S. Mohan, M.L. Baesso, Spectroscopic and glass transition studies on Nd^{3+}-doped sodium zinc borate glasses, Physica B 337 (2003) 249–254.
[18] A. Florez, J.F. Martinez, M. Florez, P. Porcher, Optical transition probabilities and compositional dependence of Judd-Ofelt parameters of Nd^{3+} ions in fluoroindate glasses, J. Non-Cryst. Solids 284 (2001) 261–267.
[19] E.O. Serqueira, N.O. Dantas, A.F.G. Monte, M.J.V. Bell, Judd-Ofelt calculation of quantum efficiencies and branching ratios of Nd^{3+} doped glasses, J. Non-Cryst. Solids 352 (2006) 3628–3632.
[20] I. Pal, A. Agarwal, S. Sanghi, M.P. Aggarwal, S. Bhardwaj, Fluorescence and radiative properties of Nd^{3+} ions doped zinc bismuth silicate glasses, J. Alloys Compd. 587 (2014) 332–338.
[21] Sk Mahamuda, K. Swapna, A. Srinivasa Rao, M. Jayasimhadri, T. Sasikala, K. Pavani, L. Rama Moorthy, Spectroscopic properties and luminescence behavior of Nd^{3+} doped zinc alumino bismuth borate glasses, J. Phys. Chem. Solid. 74 (2013) 1308–1315.
[22] B. Karthikeyan, R. Philip, S. Mohan, Optical and non-linear optical properties of Nd^{3+}-doped heavy metal borate glasses, Opt Commun. 246 (2005) 153–162.
[23] L.R.P. Kassab, N.D.R. Junior, S.L. Oliveira, Laser spectroscopy of Nd^{3+}-doped PbO-Bi_2O_3-Ga_2O_3-BaO glasses, J. Non-Cryst. Solids 352 (2006) 3224–3229.
[24] B. Karthikeyan, S. Mohan, Structural, optical and glass transition studies on Nd^{3+}-doped lead bismuth borate glasses, Physica B 334 (2003) 298–302.
[25] Y. Chen, Y. Huang, M. Huang, R. Chen, Z. Luo, M. Huang, Effect of Nd^{3+} on the spectroscopic properties of bismuth borate glasses, J. Am. Ceram. Soc. 88 (2005) 19–23.
[26] M.B. Saisudha, J. Ramakrishna, Optical absorption of Nd^{3+}, Sm^{3+} and Dy^{3+} in bismuth borate glasses with large radiative transition probabilities, Opt. Mater. 18 (2002) 403–417.
[27] B.R. Judd, Optical absorption intensities of rare-earth ions, Phys. Rev. 127 (1962) 750–761.
[28] G.S. Ofelt, Intensities of crystal spectra of rare-earth ions, J. Chem. Phys. 37 (1962) 511–520.
[29] S. Mohan, K.S. Thind, G. Sharma, L. Gerward, Specroscopic investigations of Nd^{3+} doped fluoro- and chloro-borate glasses, Spectrochim. Acta 70 (2008) 1173–1179.
[30] J. Pisaraka, W.A. Pisarski, W. Ryba-Romanowski, Laser spectroscopy of Nd^{3+} and Dy^{3+} ions in lead borate glasses, Optics Las. Technol. 42 (2010) 805–809.
[31] B. Karthikeyan, S. Mohan, S.P. Jose, Preparation and characterization of Nd^{3+} doped sodium lead bismuthate glass, Spectrochim. Acta 65 (2006) 1134–1137.
[32] J. Pisarska, W.A. Pisarski, G. Dominiak-Dzik, W. Ryba-Romanowski, Spectroscopic investigations of Nd^{3+} ions in B_2O_3-PbO-Al_2O_3-WO_3 glasses, J. Mol. Struct. 792–793 (2006) 201–206.
[33] L.C. Courrol, L.R.P. Kassab, V.D.D. Cacho, S.H. Tatumi, N.U. Wetter, Lead fluoroborate glasses doped with Nd^{3+}, J. Lumin. 102–103 (2003) 101–105.
[34] C.R. Kesavulu, H.J. Kim, S.W. Lee, J. Kaewkhao, N. Wantana, E. Kaewnuam, S. Kothan, S. Kaewjaneng, Spectroscopic investigations of Nd^{3+} doped gadolinium calcium silica borate glasses for the NIR emission at 1059 nm, J. Aloys Compd. 695 (2017) 590–598.
[35] A. Kumar, D.K. Rai, S.B. Rai, Optical properties of Nd^{3+} ions doped in oxyfluoroborate glass, Spectrochim. Acta, Part A 58 (2002) 1379–1381.
[36] G. Gupta, A.D. Sontakke, P. Karmakar, K. Biswas, S. Balaji, R. Saha, R. Sen, K. Annapurna, Influence of bismuth on structural, elastic and spectroscopic properties of Nd^{3+} doped zinc-boro-bismuthate glasses, J. Lumin. 149 (2014) 163–169.
[37] M. Shoaib, G. Rooh, N. Chanthima, T. Sareein, H.J. Kim, S. Kothan, J. Kaewkhao, Luminescence properties of Nd^{3+} ions doped ZnO-BaO-(Gd_2O_3/GdF_3)-P_2O_5 glasses for laser material applications, J. Lumin. 236 (2021), 118139.
[38] J. Pisarska, M. Soltys, A. Gorny, M. Kochanowicz, J. Zmojda, J. Dorosz, D. Dorosz, M. Sitarz, W.A. Pisarski, Rare earth-doped barium gallo-germanate glasses and their near-infrared luminescence properties, Spectrochim. Acta, Part A 201 (2018) 362–366.
[39] V. Chandrappa, Ch Basavapoornima, C.R. Kesavulu, A. Mohan Babu, D. Shobha Rani, C.K. Jayasankar, Spectral studies of Dy^{3+}:zincphosphate glasses for white light source emission applications: a comparative study, J. Non-Cryst. Solids 583 (2022), 121466.
[40] Pikkili Ramprasad, Ch Basavapoornima, Shobha Rani Depuru, C.K. Jayasankar, Spectral investigations of Nd^{3+}:$Ba(PO_3)_2$+La_2O_3 glasses for infrared laser gain media, Opt. Mater. 129 (2022), 112482.
[41] A. Renuka Devi, C.K. Jayasankar, Optical properties of Nd^{3+} ions in lithium borate glasses, Mater. Chem. Phys. 42 (1995) 106–119.
[42] K. Upendra Kumar, P. Babu, K.H. Jang, H.J. Seo, C.K. Jayasankar, A.S. Joshi, Spectroscopic and 1.06 nm laser properties of Nd^{3+}-doped K-Sr-Al phosphate and fluorophosphate glasses, J. Alloys Compd. 458 (2008) 509–516.
[43] L. Jyothi, V. Venkatramu, P. Babu, C.K. Jayasankar, M. Bettinelli, G. Mariotto, A. Speghini, Composition and concentration dependence of spectroscopic properties of Nd^{3+}-doped tellurite and metaborate glasses, Opt. Mater. 33 (2011) 928–936.
[44] S. Surendra Babu, P. Babu, C.K. Jayasankar, A.S. Joshi, A. Speghini, M. Bettinelli, Luminescence and optical absorption properties of Nd^{3+} ions in K-Mg-Al phosphate and fluorophosphate glasses, J. Phys. Condens. Matter 18 (2006) 3975–3991.
[45] D.L. Dexter, A theory of sensitized luminescence in solids, J. Chem. Phys. 21 (1953) 836–850.
[46] Th Förster, Intermolecular energy migration and fluorescence, Ann. Phys. 2 (1948) 55–75.
[47] T. Kushida, Energy transfer and cooperative optical transitions in rare-earth doped inorganic materials. I. Transition probability calculation, J. Phys. Soc. Jpn. 34 (1973) 1318–1326.
[48] M. Inokuti, F. Hirayama, Influence of energy transfer by the exchange mechanism on donor luminescence, J. Chem. Phys. 43 (1965) 1978–1989.